Influence of the Wall Thicknesses on the Joint Quality During Magnetic Pulse Welding in Tube-to-Tube Configuration

J. Lueg-Althoff[1*], B. Schilling[1], J. Bellmann[2,3], S. Gies[1], S. Schulze[3], A. E. Tekkaya[1], E. Beyer[2,3]

[1] Institute of Forming Technology and Lightweight Construction, TU Dortmund University, Germany
[2] Institute of Manufacturing Technology, TU Dresden University, Germany
[3] Fraunhofer Institute for Material and Beam Technology, Dresden, Germany
[*]Corresponding author. Email: Joern.Lueg-Althoff@iul.tu-dortmund.de

Abstract

The implementation of multi-material concepts, for example, in automotive engineering or aerospace technologies, requires adequate joining techniques. The Magnetic Pulse Welding (MPW) process allows for joining both similar and dissimilar materials without additional mechanical elements, chemical binders, or adverse influences of heat on the joining partners. In this process, an electro-conductive at ('flyer') part is accelerated by Lorentz forces and impacts the inner ('parent') part under high velocity and high pressure, leading to the formation of a metallurgical joint. Besides joining of sheets and tubes to solid cylinders, the connection of two tubes is of particular interest due to the increased lightweight potential. The present paper focuses on the MPW of aluminum (EN AW-6060) to steel (C45) tubes. An experimental study was performed, in which the wall thickness of the parent part was reduced successively. The deformation behavior of both the flyer and parent parts was recorded during the experiments by a two-probe Photon Doppler Velocimeter (PDV). The final shape of the joined specimens was analyzed by a 3D digitizer. An instrumented peel test was used for the determination of the weld quality. It was found that defect-free MPW of aluminum tubes on steel tubes without supporting mandrel is possible.

Keywords

Joining, Welding, Magnetic pulse welding

1 Introduction

Lightweight design concepts pursue the objective to reduce the weight of components without decreasing their functionality. For example, solid cylinders are replaced by hollow parts whenever possible. In material lightweight concepts, the aim is to choose the optimum material for every single component of a structure. Considering this background, the combination of the described concepts leads to an increasing demand of joining weight optimized parts made from different materials (Gude et al., 2015). Especially the joining of materials with very different physical properties (e.g., melting point and thermal conductivity) is challenging for conventional thermal joining techniques. In many cases, thermally induced defects like cracks and distortion cannot be avoided (Kapil and Sharma, 2015).

Magnetic Pulse Welding (MPW) is an impact welding process used to create solid-state joints without adverse influence of heat. The joint results from the collision of the joining partners at a certain angle β at radial impact velocities v_r of up to several hundred m/s and pressures of up to a few thousand MPa. Flat or tubular overlap joints can be fabricated, allowing for the application as a joining process for frame structures or torque tubes (Mori et al., 2013). **Fig. 1** explains the MPW process using the example of a tube-to-tube connection made by electromagnetic compression showing the basic process principle (b), a schematic illustrating the processes at the collision line (a), and an example aluminum-steel joint (c). The process variant of MPW by electromagnetic compression is the one investigated within the presented study.

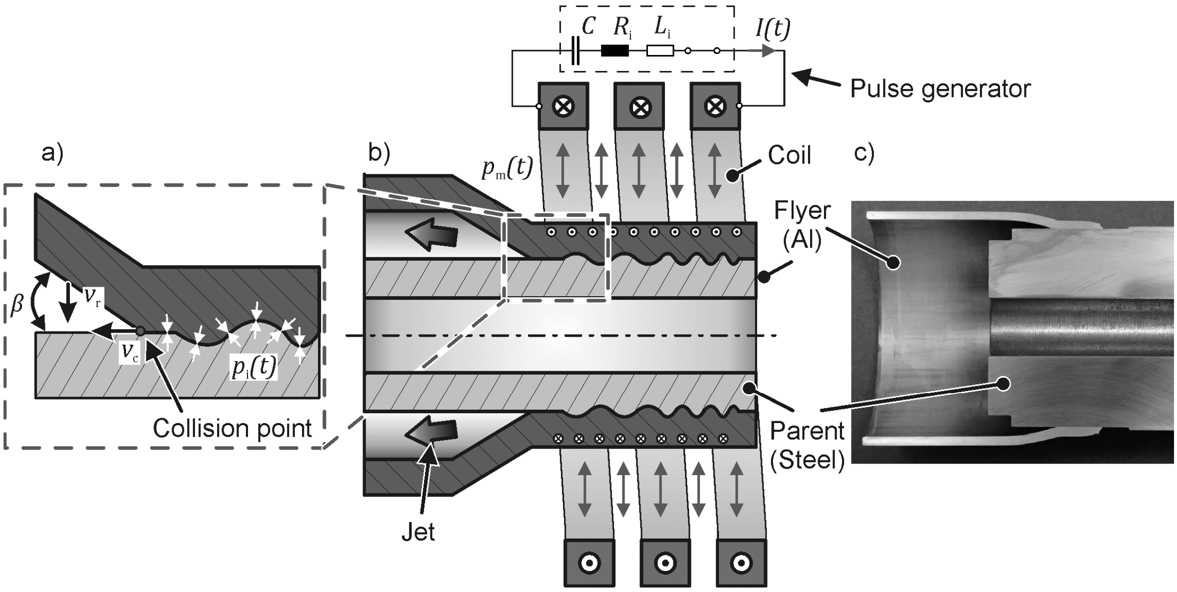

***Figure 1**: a) Processes at the collision zone, b) Process principle of magnetic pulse welding, c) Example of an aluminum-steel joint*

In the following, the MPW process is described briefly. The electric energy stored in a capacitor bank is discharged within several microseconds through a compression coil resulting in a damped sinusoidal current of several hundred kiloamperes. The accompanying magnetic field induces an opposing secondary current in the electroconductive outer workpiece, the so-called flyer. Lorentz forces, which can mathematically be described by the magnetic pressure $p_m(t)$, are created between coil and flyer resulting in an acceleration of the flyer as soon as the yield stress of the material is exceeded. The flyer and the fixed inner part ('parent') collide under high pressure and at high velocities. The rapid movement of the collision front leads to the formation of a so-called "jet", which cleans the surfaces of the joining parts and leaves them chemically pure, favoring the creation of metallic bonds under the prevailing interface pressure $p_i(t)$.

Due to the mentioned advantages in combination with many unsolved questions, MPW has caused an increasing interest among research institutes and industrial users in recent years. Very active research fields are the expansion of weldable material combinations, the in-depth analysis of the relevant process parameters, an improvement of the tools with regard to durability and numerical simulations to enlighten the actual joining mechanism. (Kapil and Sharma, 2015)

Great effort has been put into analyzing the influence of surface characteristics like roughness (Geyer et al., 2014) and the geometric features of the flyer part, e.g., the wall thickness. However, several researchers have shown interest in the characteristics of the parent. Ben Artzy et al. related the thickness of the parent part to the shockwave characteristics and the interfacial wave formation (Ben-Artzy et al., 2010).

Tamaki and Kojima (1988) investigated several parameters of the MPW process with aluminum flyer tubes (29 mm outer diameter, 1 mm wall thickness) on aluminum parents with different wall thicknesses. They found out, that with an increasing wall thickness of the parent part, the weld quality (defined as the ratio of the welded portion along the circumference to the circumference; measured by peel testing) increases from approx. 50 % at 2 mm up to 100 % for wall thicknesses greater 6 mm. The reasons for this observation were not investigated.

Cui et al. (2016) presented a study of tube-to-tube MPW with aluminum flyer and steel parent (flyer: 20 mm outer diameter, 1 mm wall thickness; parent: 15.2 mm outer diameter, 1.5-4 mm wall thickness). They define a critical parent tube thickness depending on the discharge voltage. Below the critical thickness value, tensile testing of joints results in a separation at the welding zone. Above the critical value the joint fails in the base aluminum. The authors present an analytical approach for the calculation of the plastic deformation of the inner part based on Lame's equations for the stresses in tubes depending on the acting inner and outer pressures.

Usually, joining by forming of tubular workpieces is performed with the help of stabilizing mandrels inserted into the parent part (e.g., Weddeling, 2015). This prevents a deformation of the parent but has the risk of jamming after the process. The objective of this paper is to analyze the deformation behavior of the unsupported parent part and to provide guide values for mandrel-free MPW in tube-to-tube configuration.

2 Experimental Setup

2.1 Materials and Tools

The deployed flyer parts had an outer diameter of 40 mm and wall thicknesses s_f of 1.5 and 2 mm. They were manufactured out of EN AW-6060 (T66), which is a common alloy for various lightweight applications. Selected tubes were heat-treated at 500 °C for 1 h with subsequent air cooling in order to reduce the strength. The measured yield stress was 60 MPa in the heat-treated and 222 MPa in the T66 state, determined by tensile tests. The parent tubes out of C45 steel had an outer diameter of 32, 33, or 34 mm and a wall thickness s_p of 1-8 mm. The initial standoff a between flyer and parent was 1.5 and 2 mm, respectively. **Fig. 2a** illustrates the geometrical setup.

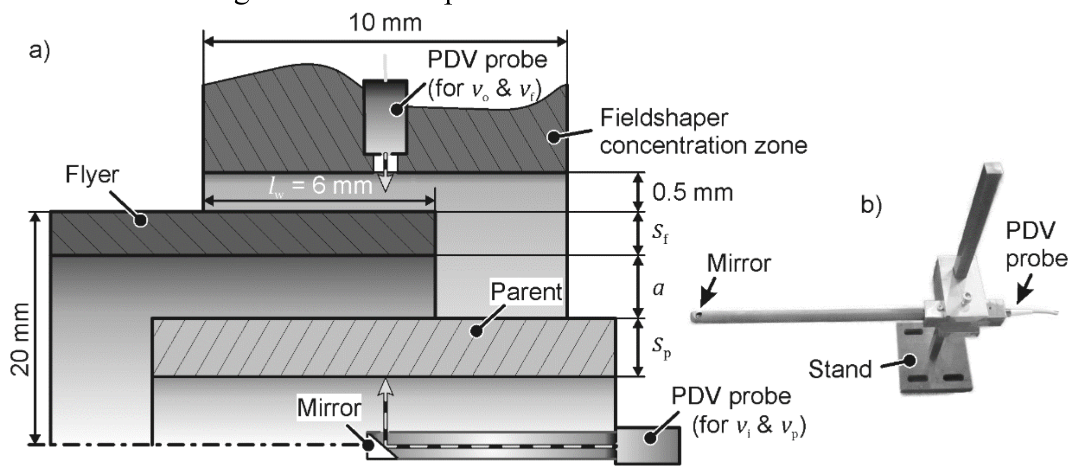

***Figure 2**: a) Experimental setup and PDV measurement devices, b) PDV periscope*

MPW experiments at various discharge energy and frequency levels were performed with a Maxwell Magneform 7000 32 kJ pulse generator. This machine consists of four capacitor banks with different characteristics, which can be used in variable combinations, influencing the properties of the discharge current. The bank configurations 2+3 (A) and 3+4 (B) were used during this study, see **Table 1**. An eight-turn compression coil with an inner diameter of 97 mm and a length of 90 mm in combination with a fieldshaper with a 10 mm long concentration zone and an inner diameter of 41 mm was used. The working length l_w was set at 6 mm.

	Maxwell Magneform A (Bank 2+3)	Maxwell Magneform B (Bank 3+4)
Max. charging energy E_{max}	12 kJ	8 kJ
Max. charging voltage U_{max}	8.16 kV	8.16 kV
Inner capacitance C_i	362 µF	251 µF
Inner inductance L_i	78 nH	100 nH
Inner resistance R_i	5.4 mΩ	6.8 mΩ
Resonant frequency f^*	29 kHz	31 kHz

***Table 1**: Characteristics of the pulse generator configurations*

2.2 Measurement Technology

Coil current measurements were conducted for each trial using a Rogowski current probe CWT 3000 B from Power Electronic Measurements Ltd. For recording the radial impact velocities v_r and calculating of the final displacement h, a collimator style PDV probe was integrated into the concentration zone of the fieldshaper (Fig. 2a). This idea was first presented by Jäger and Tekkaya (2012) and the concept proved to be suitable for measuring the velocities in MPW experiments (e.g., Lueg-Althoff et al., 2014). In that reference, the technical details of the applied PDV system are described. The deformation behavior of the parent part was monitored by a second, focuser style PDV probe (**Fig. 2b**). The laser beam was directed onto the inner parent surface at the area of impact by a mirror made of polished aluminum, which deflects the laser beam at 90°, see Fig. 2.
The welded specimens were mechanically tested with an instrumented 90° peel testing device integrated into a Zwick Z250 tensile testing machine (see Hahn et al., 2016 for the testing setup) and a straight tensile test. Selected welded specimens were digitized by a GOM ATOS 3D digitizer and micrographs of the joint zone were investigated with a Zeiss Axio Imager.M1m optical microscope.

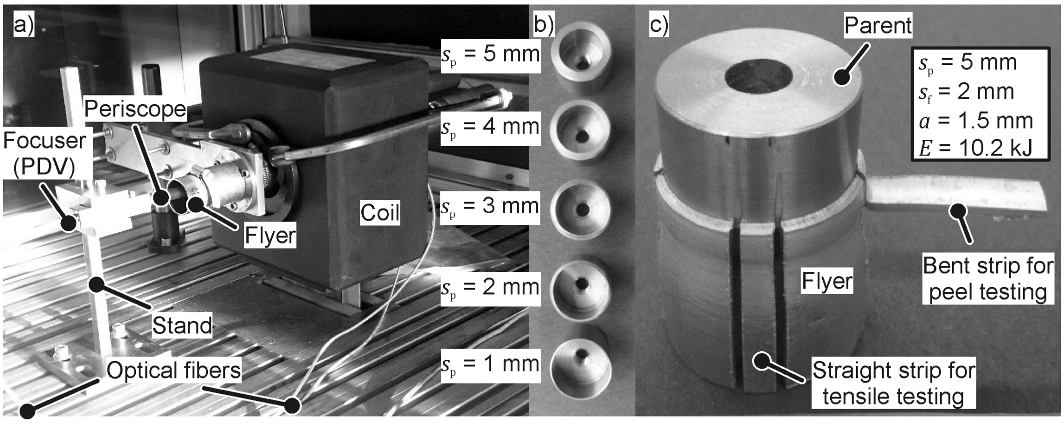

***Figure 3**: a) Experimental setup, b) Parent parts, c) Joined specimen*

3 Results and Discussion

3.1 Calibration Experiments

The parameters for the experiments were chosen on the basis of successful MPW experiments with solid parent parts and were adapted to the thickness of the flyer part. For every trial, the discharge current $I(t)$ and the PDV recordings were evaluated. The capacitor bank configuration of the pulse generator was chosen in a way that allowed high enough current amplitudes as well as discharge frequencies. The positioning of the periscope PDV probe was done in free compression experiments. **Fig. 4a** shows the result of PDV measurements of a free compression experiment of an aluminum tube (heat-treated state, wall thickness 2 mm) at 3.2 kJ in bank configuration B. There is a sufficient agreement between the graphs for the inner and the outer tube surface, which confirms that the measurement was performed at the same axial position. The deviation between the peak velocities is 3.4 %.

Fig. 4.b shows example current and PDV curves of an MPW experiment; only the first half wave of the current path is depicted at 5.6 kJ (Maxwell configuration B). It can be seen that the acceleration of the flyer begins shortly after the current rises and that it impacts the parent after approx. 15 µs. At this moment, the periscope PDV probe starts recording a movement of the parent part surface. The first peak of the parent part movement is regarded as a measure for the deformation of the parent part. The peak velocity of flyer $v_{f,max}$ and parent $v_{p,max}$ were set into relation for further investigations.

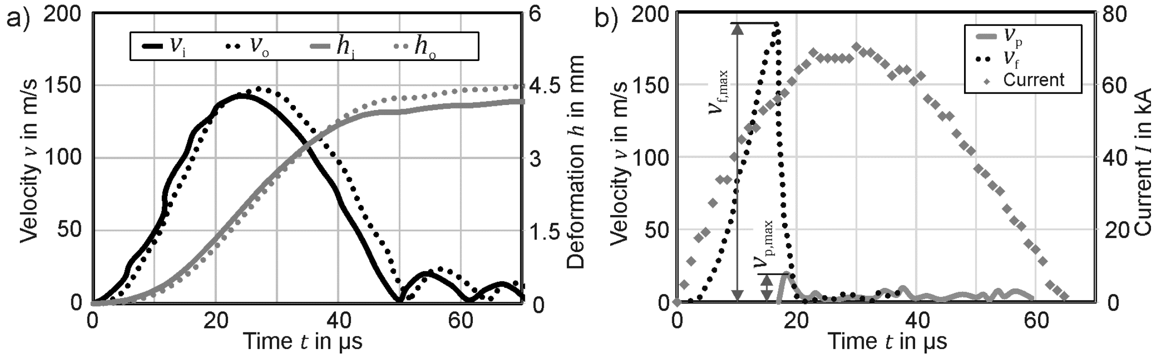

***Figure 4**: a) Measured velocity for a free compression experiment at 3.2 kJ, b) Measured current and velocity curves for an MPW experiment at 5.6 kJ*

3.2 Variation of Discharge Energy

In a first set of experiments, welding trials with a fixed flyer wall thickness s_f and standoff a of 2 mm were performed under varying discharge energies and a fixed discharge frequency of 8.7 kHz. **Fig. 5a** shows that an increase of the discharge energy (bank configuration B) leads to an increase of both the velocity of the flyer and the deformation velocity of the parent. The variations of the values at the same energies result from inaccuracies of the relative radial positioning of flyer to parent.

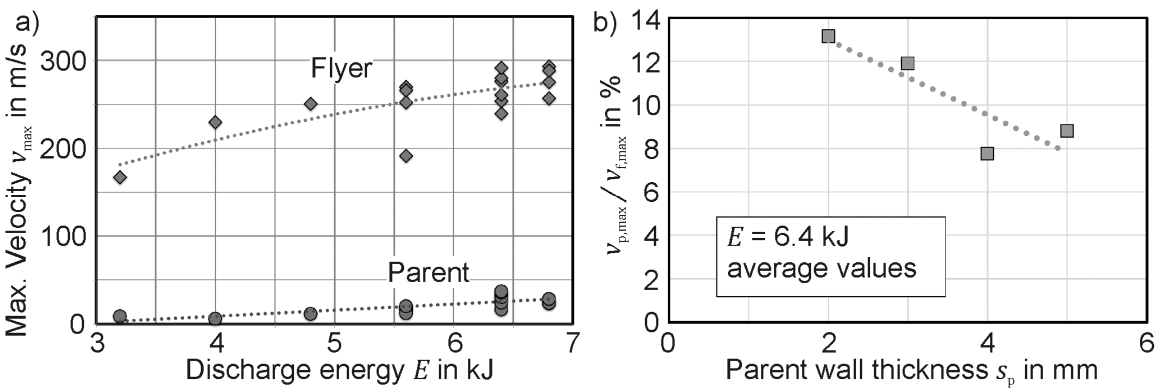

***Figure 5**: a) Peak velocities depending on the discharge energy, b) Ratio of* $v_{p,max}$ *and* $v_{f,max}$ *depending on the parent wall thickness*

Fig. 5b shows that a decrease of the parent wall thickness s_p leads to an increase of the parent deformation velocity and, thus, to an increase of the ratio $v_{p,max}$ and $v_{f,max}$. It is not possible to determine if the parent is elastically or plastically deformed on the basis of the velocity curve alone. In order to answer this question, selected specimens were digitized with a 3D scanner and the inner contour of the parent part after MPW was compared to a perfect cylinder, see **Fig. 6**. For parent wall thicknesses s_p greater than 3 mm (Fig. 6a), no permanent deformation of the parent was observed. A further reduction of s_p still allows welding to take place; in Fig 6b, residual strips of the flyer material can be seen. However, the parent part experiences a permanent reduction of the radius in the area of impact of up to 0.23 mm. This zone is not distributed uniformly around the circumference due to the non-uniform field distribution (fieldshaper slot) and the mentioned inaccuracies in positioning.

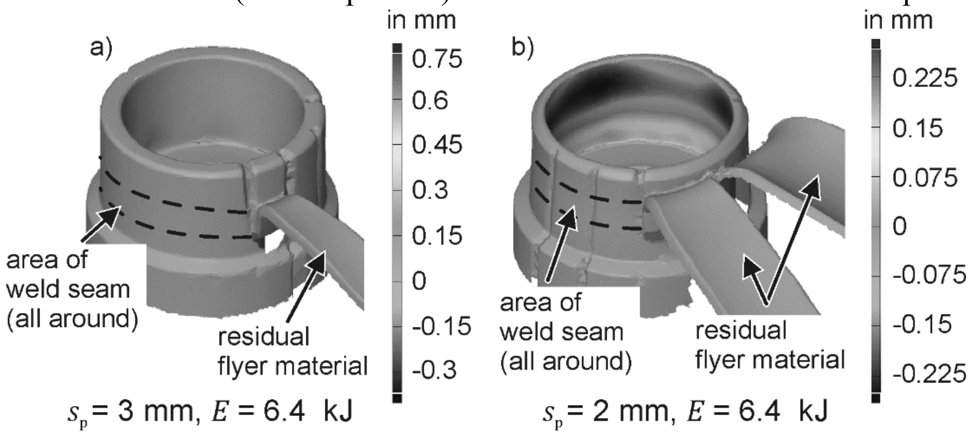

***Figure 6**: 3D scans of parent parts after MPW, Deviation compared to a perfect cylinder*

a)

s_p in mm	E in kJ	Proof stress $R_{p0.01}$ in MPa	Tensile stress R_m in MPa
5	5.6	50	61
4	6.4	105	146
4	6.4	92	98
3	6.4	82	120
3	6.4	72	87
3	6.8	95	113
2	6.4	104	147
2	6.8	68	78

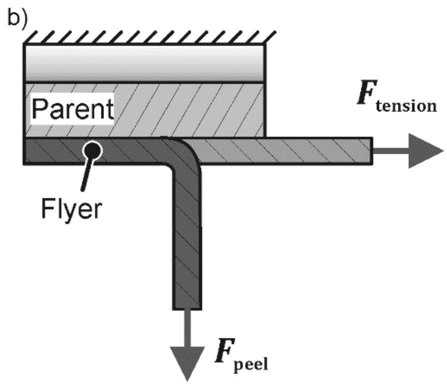

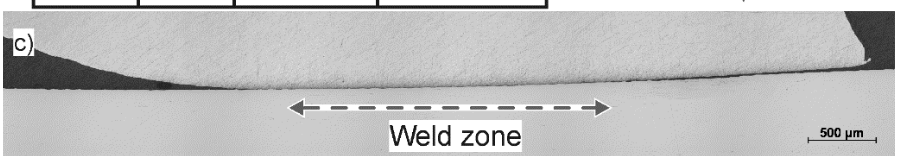

***Figure 7**: a) Results of tensile test, b) Schematic for tensile and peel test, c) Micrograph of welded specimen*

The quality of the welding results was determined in tensile tests. Strips with a width of approx. 6 mm were axially cut off the specimens. The specimens were clamped in a

Zwick Z 250 tensile testing machine and then axially loaded with a tension force. The force and the displacement were recorded. **Fig. 7a** shows that, for the given parameters, successful welding in tube-to-tube configuration by MPW is feasible without using supporting mandrels. The proof stress exceeds the flow stress of the aluminum alloy due to strain hardening mechanisms. The micrograph of a specimen with s_p = 2 mm (**Fig. 7c**, specimen refers to shaded row in Fig. 7a) shows an approx. 2.5 mm weld zone starting approx. 2 mm from the free flyer edge.

3.3 Variation of Flyer Material, Flyer Wall Thickness, Initial Standoff and Discharge Frequency

In a second set of experiments based on the previous results, several other process parameters were varied. All experiments were carried out in a capacitor bank configuration B (see Table 1), which allows higher discharge energies but limits the discharge frequency to 7.1 kHz. Two different flyer wall thicknesses s_f were used (1.5 and 2 mm). The experiments with s_f = 1.5 mm were performed with an initial standoff a = 2 mm and a discharge energy E of 9.6 kJ, those with s_f = 2 mm were performed with a = 1.5 mm and E = 10.2 kJ. The thickness of the parent part s_p was varied between 1 and 5 mm. **Fig. 8** summarizes the results of the velocity measurements. As seen before, the maximum deformation velocity $v_{p,max}$ of the parent part rises with decreasing s_p. The flyer parts out of the softer, heat-treated material reach approx. 10 % higher impact velocities than those in T66 state, which leads to higher deformation velocities of the parent parts and thus to an increasing ratio of $v_{p,max}$ / $v_{f,max}$ (Fig. 8). The increasing velocity ratio is also reflected by an increasing deformation of the parent part.

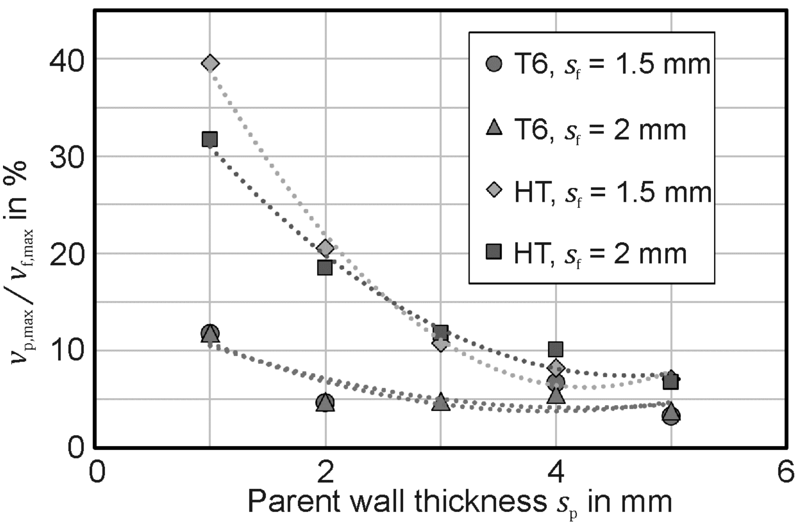

***Figure 8**: Velocity measurements for the second set of experiments, HT = heat treated*

The specimens in T66 state did not undergo welding. Apparently, the reached impact velocities (maximum of 240 m/s for the 1.5 mm specimens) were not high enough for metallurgical bonding. The heat-treated specimens underwent welding and were tested in a 90°

peel test, which applies a very severe loading perpendicular to the weld seam. **Fig. 9a** summarizes the results of this test, the stress values correspond to the width and the thickness of the metal strips. Due to the specific force application, the stress values are below the ones of the 0° tensile test. For the specimen marked with *, the peel test had to be stopped due to a beginning plastic deformation of the parent. The parent parts with s_p = 1 mm wall thickness deformed heavily during the experiments (see **Fig. 9b**), the flyer was basically crimped onto the parent, the joint failed under low loadings.

a)

s_p in mm	s_f in mm	Maximum stress in MPa
5	1.5	56
4	1.5	56
3	1.5	52
5	2	96
4	2	34
3	2	40
2	2	79*

b)

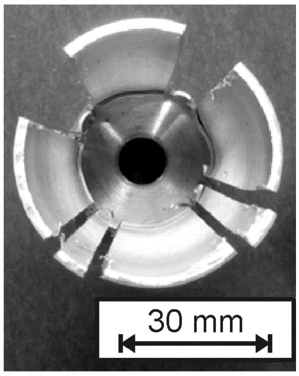

***Figure 9**: a) Results of 90° peel test, flyers were in heat-treated state, b) Deformed thin-walled parent part*

4 Conclusions and Outlook

- A periscope-style PDV probe was developed and successfully applied for inline measurement of the deformation of hollow parent parts in MPW.
- Thin-walled steel parent parts of down to the thickness of the aluminum flyer part can be welded by MPW without supporting mandrel.
- Parent wall thicknesses smaller than that of the flyer lead to plastic deformation of the parent, but welding can still be achieved.
- On the basis of the presented study, an estimation of the deformation of hollow mandrels with specific wall-thickness during MPW can be conducted.

For future investigations, an analytical correlation of mechanical parameters of the parent material and the impact conditions is planned in order to predict the deformation behavior. Existing models of shock wave propagation and their influence on the weld formation should be reviewed for the given setup.

Acknowledgments

The presented results originate from research carried out within the subproject A1 of the priority program 1640 (“joining by plastic deformation”) funded by the German Research Foundation (DFG). The financial support is greatly acknowledged.

References

Ben-Artzy, A., Stern, A., Frage, N., Shribman, V., Sadot, O., 2010. Wave formation mechanism in magnetic pulse welding. International Journal of Impact Engineering 37 (4), pp. 397–404.

Cui, J., Sun, G., Xu, J., Xu, Z., Huang, X., Li, G., 2016. A study on the critical wall thickness of the inner tube for magnetic pulse welding of tubular Al–Fe parts. Journal of Materials Processing Technology 227, pp. 138–146.

Geyer, M., Rebensdorf, A., Böhm, S., 2014. Influence of the boundary layer in magnetic pulse sheet welds of aluminium to steel. In: Huh, H., Tekkaya, A.E. (Eds.), High Speed Forming 2014, Proceedings of the 6th International Conference, Daejeon, Korea, pp. 51-60.

Gude, M., Meschut, G., Zäh, M.F., Lieberwirth, H., 2015. Chancen und Herausforderungen im ressourceneffizienten Leichtbau für die Elektromobilität – FOREL-Studie, http://plattform-forel.de/wp-content/uploads/2015/05/FOREL-Studie.pdf

Hahn, M., Weddeling, C., Lueg-Althoff, J., Tekkaya, A.E, 2016. Analytical approach for magnetic pulse welding of sheet connections. Journal of Materials Processing Technology 230, pp. 131–142.

Jäger, A., Tekkaya, A.E., 2012. Online measurement of the radial workpiece displacement in electromagnetic forming subsequent to hot aluminium extrusion. In: Tekkaya, A.E., Daehn, G.S., Kleiner, M. (Eds.), High Speed Forming 2012, Proceedings of the 5th International Conference, Dortmund, Germany, pp. 13-22.

Kapil, A., Sharma, A., 2015. Magnetic pulse welding: an efficient and environmentally friendly multi-material joining technique. Journal of Cleaner Production 100, pp. 35-58.

Lueg-Althoff, J., Lorenz, A., Gies, S., Weddeling, C., Göbel, G., Tekkaya, A.E, Beyer, E., 2014. Magnetic pulse welding by electromagnetic compression: Determination of the impact velocity. Advanced Materials Research 966-967, 489–499.

Mori, K., Bay, N., Fratini, L., Micari, F., Tekkaya, A.E., 2013. Joining by plastic deformation. CIRP Annals – Manufacturing Technology 62 (2), pp. 673-694.

Tamaki, K., Kojima, M., 1988. Factors affecting the result of electromagnetic welding of aluminum tube. Transactions of the Japan Welding Society 19 (1), 53–59.

Weddeling, C., 2015. Electromagnetic Form-Fit Joining, Dr.-Ing. Dissertation, Dortmund, Germany.